



Open Archive TOULOUSE Archive Ouverte (OATAO)

OATAO is an open access repository that collects the work of Toulouse researchers and makes it freely available over the web where possible.

This is an author-deposited version published in : <http://oatao.univ-toulouse.fr/>
Eprints ID : 18196

To link to this article : DOI: 10.1109/ESTC.2016.7764674
URL : <http://dx.doi.org/10.1109/ESTC.2016.7764674>

To cite this version : Pin, Samuel and Frémont, Hélène and Gracia, Alexandra *Numerical study of thermomechanical fatigue influence of intermetallic compounds in a lead free solder joint.* (2016) In: ESTC 2016 (6th Electronics System-Integration Technology Conference), 13 September 2016 - 16 September 2016 (Grenoble, France).

Any correspondence concerning this service should be sent to the repository administrator: staff-oatao@listes-diff.inp-toulouse.fr

Numerical study of thermomechanical fatigue influence of intermetallic compounds in a lead free solder joint.

S. Pin^{1,2}, H. Frémont², A. Gracia²

¹ Institut de Recherche Technologique Saint-Exupéry, 118 Route de Narbonne, 31432 Toulouse, France ;

² Université de Bordeaux, IMS UMR 5218, 351, cours de la Libération, 33405 Talence Cedex, France

Abstract

The study aims at investigating the influence of IMC growth on the thermomechanical fatigue behaviour of lead free solder joints. As a potential driving parameter of the failure of such assemblies, a numerical study is carried out to conclude on the implementation in future predictive FE models. A first FE model of a Single Lap Shear test is used to highlight in which conditions neglecting the IMC thickness can be an issue for material identification. It has been shown that common IMC layers present after fusion do not represent an important source of error except for the thinnest and stiffest soldered joints. The most important impact of IMC on this kind of test is the error of estimation on the Young's modulus and the stress increasing at the ends of the joint. The creep properties determination is not impacted by IMC. A second FE model is used to simulate the consequences of IMC growth in a BGA. The simulation of a classic BGA under a thermal load shows that warpage is not really impacted by a stiffer joint contrary to the stress levels in the corner ball. Differential displacement due to CTE mismatch produces higher stress levels in the solder balls near the bi-material interfaces when IMC layers are considered. Submodelling techniques are used to analyse with more details the interfacial gradients of stress and determine if IMC implementation is necessary to reproduce all the potential conditions of failure.

Introduction

As electronics is increasingly present, the reliability of automotive and aircraft equipment is linked to the reliability of electronic boards. Solder bumps are subjected to multiple stresses (e.g. mechanical, thermal, thermo-mechanical, coupled electro-thermal) due to usage conditions. In the scope of RoHS directive [1], solder joints are made of lead-free alloys. Very promising candidates for replacing standard SnPb solders in electronic assemblies, they are based on Tin-Silver-Copper alloys, commonly referred to as SAC.

In a more global scope of fatigue characterisation of lead-free solder joints, the main objective is to identify relevant fatigue mechanisms involved. Two common ways are usually chosen: fitting a fatigue law after a campaign of thermal cycling or extracting a fatigue parameter from finite elements (FE) analyses that is relevant with experimental observation of the failure [2].

According to literature, the second method is intimately linked to the representativeness of FE models. Before using them for prediction, they must be somehow correlated with measurements [3]. In order not to neglect any influent

factor involved in the mechanical behaviour of the joint, the role of some parameters must be determined.

Among geometric or metallurgic parameters, the intermetallic compound (IMC) growth is of great concern because of its sensitivity to the temperature as well as its mechanical drawbacks on the solder joint. The IMC come from the reaction between the alloy and the finishes. They grow at high temperatures when atomic diffusion mechanisms are activated [4] i.e. during reflow and thermal cycling. IMC are also stiffer and more brittle than both SnPb and lead free alloy [5], [6]. IMC geometry and material affect the thermo-mechanical performance of micro-joints [7] as well as more classical solder bumps [8]. They have hence to be taken into account in the numerical fatigue assessment, as they will change the fatigue behaviour of the whole assembly.

Usually, fatigue studies involving FE simulations are based on a fatigue variable, as the dissipated energy or the plastic strain for instance. Often it leads to an assessment of fatigue life by the calculation of a plastic strain accumulation averaged in the most loaded region [9]. Hence, it requires specific material behaviours and a detailed geometry. Similarly, it would be interesting to study failure initiation due to IMC if relevant by implementing a proper material behaviour in a representative model with IMC. At the end, the study of stress concentrations in the vicinity of IMC layers could help to identify a fatigue scenario with regards to the thermal history of the assembly.

To achieve this goal, it is necessary to get the proper mechanical behaviour of the assembly. As highlighted in [10], some discrepancies are deplored among the material properties available in literature. It is mainly due to differences in the characterisation methodology. It is globally accepted that the right way to get the material behaviour is to test specimens close to the application configuration in terms of volume and reflow temperature profile. The aim is to obtain the same microstructure with the right amount of intermetallic compounds.

The issue for such small specimens is the sensitivity of the results to different parameters like measurement, solicitation modes, or homogeneity. Reduced volumes of alloy also imply a larger part of the stiffness accounted for IMC. Therefore, the first part of this work deals with the investigation of the conditions to meet during a single lap shear test to avoid an important error on the material characterisation.

The second part of this work deals with the impact of IMC layers on the locations of stress concentrations for two BGA configurations: Non Solder Mask Defined and Solder Mask Defined.

Single Lap Shear test considerations

A specific geometry of single lap shear specimen has been selected for SAC characterisation. They are grooved specimens adapted from Iosipescu's works [11]. [12] justified the benefits of such a test for thin joints.

The campaign of characterisation will start with classic monotonic shear tests to get the principal properties of the solder material: Young's modulus, yield stress, ultimate stress, etc. As a second step, creep tests performed at different temperatures will allow the identification of a Garofalo-like material behaviour.

To get the most uniform shear field across the joint and reduce peeling stress levels at the ends, the geometry (grooves depth) was numerically optimised (Fig. 1). The model also enables to evaluate the impact of IMC from interfaces on such tests. Questions to be answered are the following ones: is there a significant shift on the results because of IMC growth? is it measurable? what is the impact on creep properties?

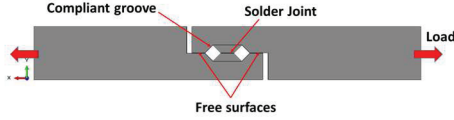


Fig. 1 : SLS specimen with grooves

A 2D finite element model of the specimen was made on ABAQUS. A solicitation is imposed on one end while the other end is fixed. The absence of degree of freedom due to the clamps during the real shear test is made by constraining the loading point in orthogonal displacement to keep its initial alignment. It reproduces the resulting moment in the assembly due to the asymmetric nature of a single lap shear specimen (Fig. 2). This side effect is reduced by taking wide bars to align external loads as proposed in [13], and [14]. However, a small rotation added to the strain of the Invar bars themselves remains. The instrumentation of this test is of great concern for the quality of the results. As an extensometer is most likely to be used for convenience, a preliminary study must determine if it will be adapted to this test or if other method like image correlation would be necessary. It consists in extracting nodal displacements from the simulations at 6 mm from either side of the joint to be representative of a measurement made with an extensometer as illustrated in Fig. 2.



Fig. 2 : Residual rotation and axis of measurement of spreading u (mm)

As the lap shear test results depend on the stiffness of the bars, their elastic modulus has to be fairly higher than the one of the tested material. Otherwise, the bars' strain is accounted in the measurement and the solder modulus is underestimated.

A batch of simulations was performed for different joint and IMC thicknesses corresponding to the thickness

of a layer at an interface. They consist in static calculations for a tensile load of 500 N applied on the end of the specimen with elastic properties only. The section of the solder joint is constant throughout the simulations, hence the unique stress carried by the solder material is equal to 20 MPa.

Average values of the Young's moduli and Poisson's coefficients available in literature [15] have been used while waiting for experimental data (Table 1).

| | Young's modulus (GPa) | Poisson's coefficient |
|-------|-----------------------|-----------------------|
| SAC | 50 | 0.3 |
| IMC | 100 | 0.3 |
| Invar | 150 | 0.3 |

Table 1 : Material properties [15]

It is possible to get an estimation of the global shear modulus IMC/Solder/IMC by applying the Rule of Mixture as extensively used for composites (1):

$$G_{eq} = \frac{G_1 G_2}{V_1 G_2 + V_2 G_1} \quad (1)$$

where G_{eq} , is the equivalent shear modulus from the mixture of G_1 , G_2 for volume fractions of V_1 and V_2 respectively. Fig. 3 gathers the equivalent bulk moduli for the different cases considered in this study. To compare these predicted values to the ones estimated from an extensometer, the relative gap of the bars is estimated, by extracting nodal displacements at the midline of the bars at 6 mm from both side of the joint. Then shear strain is calculated by dividing this spreading distance by the height of the volume in shear (the extensometer height). Out coming Young's moduli are represented with thick lines in the bar diagram given in Fig. 3 for each case.

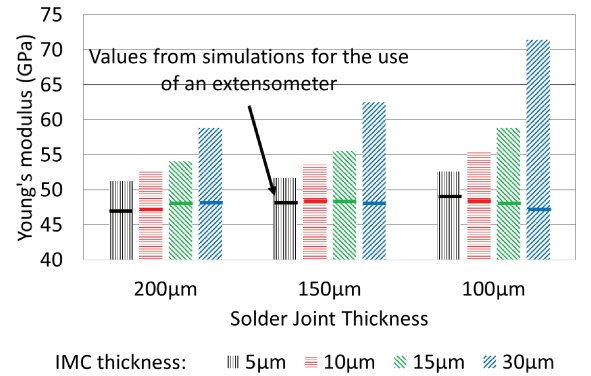


Fig. 3 : Estimated Young's moduli following the Rule of Mixture compared to measurable values using an extensometer at 6 mm from either sides of the joint

As expected, the joint stiffness increases with the IMC thickness accordingly to the IMC ratio. It can cause a shift from approximately 2 to 40% for the worst cases. This is not an issue if the IMC thickness is known because a correction could be applied on the measurements using the RoM approach. But it can be an issue if the method of measurement adds an error due to the assembly stiffness. As a matter of fact, for thin solder joints, the effect of IMC growth leads to an increase in the joint stiffness and thus to

an accumulation of strain of the bars themselves. Tensile strain in the loading direction and shear strain within the bars are responsible for the measurement error. To avoid this side effect of such a specimen, it is necessary to measure as close as possible to the bonding interfaces.

The second step of the campaign of characterisation aims at identifying the complete creep behaviour of the solder. In order to estimate to which extent the creep properties can be falsely identified, creep data from [16] are implemented in the solder joint of the single lap shear specimen model (Table 2).

| Parameter | Value | Parameter | Value |
|-----------|----------------------------------|----------------|----------------------|
| s_0 | 1 MPa | h_0 | 3090 MPa |
| Q/R | 8400 K | $\hat{\sigma}$ | 1.04 MPa |
| A | $4.61 \cdot 10^6 \text{ s}^{-1}$ | n | $4.60 \cdot 10^{-3}$ |
| ξ | 0.038 | a | 1.56 |
| m | 0.162 | | |

Table 2 : Anand's parameters [16]

Fig. 4 shows the evolution of the displacement extracted from either side of the joint with respect of time during a creep test. It shows an increasing gap between the two bars as the solder joint accumulates creep under constant shear stress. It seems that IMC thickness have an impact on the magnitude of the phenomenon.

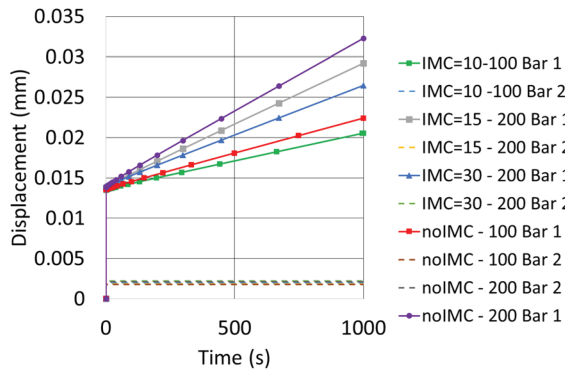


Fig. 4 : Displacement of the bars during a creep test of 500N of constant load

Then, the displacement accumulated beyond the elastic part is divided by the true thickness of solder to get the creep strain. After this manipulation, the same deformation profile is repeated with a small shift from one case to another of less than 0.1% of variation.

As for Young's moduli estimations, the error will arise from the unknown amount of IMC involved in the joint during creep tests. Careful measurements and micrographic analyses after test for IMC thickness measurement are recommended.

Ball Grid Array stiffness

The growth of IMC at the top and bottom interfaces of a solder ball increases its stiffness. To characterise the IMC impact on the mechanical response of a solder ball it is necessary to consider the whole BGA package. The global stiffness will rise and modify the way the other balls are

loaded. A quick simulation of an isolated ball shows an increase in its own stiffness up to 15%.

It can influence the loading of the balls. Fig. 5 shows the BGA package modelled in ABAQUS. It is a quarter of assembly of 144 balls of 300 μm in diameter and 800 μm of pitch.

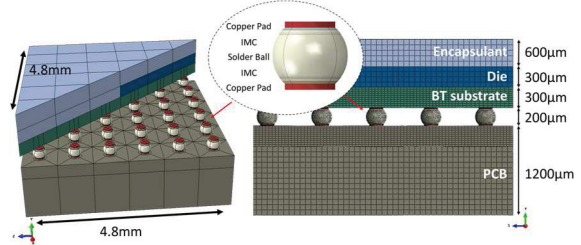


Fig. 5 : Geometry of a quarter BGA

The silicon die is perfectly bonded to a BT substrate of the same thickness. The whole stack is encapsulated by a moulding compound. PCB is made of FR4. Only SAC and the moulding material are temperature dependent in this model. Properties are taken from [16] and [17] and are listed in Table 3.

| Material | Young's modulus (GPa) | Poisson's ratio | CTE (ppm/°C) |
|-------------------|-------------------------------------|----------------------------|-----------------------------------|
| FR4 substrate | 22 (x,z) 10 (y) | 0.28 (xy,zy) 0.11 (xz) | 18 (x,z) 70 (y) |
| Copper | 120 | 0.35 | 17 |
| BT substrate | 26 (x,z) 11 (y) | 0.39 (xy, zy) 0.11 (xz) | 15 (x,z) 52 (y) |
| Si die | 131 | 0.28 | 2.8 |
| Moulding compound | 10, 25<T<165°C 1, 175<T<230°C | 0.25 | 14, 25<T<165°C 68, 175<T<230°C |
| SAC | 50, 25°C 45, 125°C 0.1, 230°C | 0.35 | 22 |

Table 3 : Material properties [16], [17]

Solder balls are modelled in two configurations: Solder Mask Defined (SMD) and Non Solder Mask Defined (NSMD). The IMC thickness is modelled by a layer of finite elements at the interfaces. The ball is coarsely meshed to allow reasonable calculation time.

Two cases, with and without IMC, are tested in each soldering configuration. The mechanical response is then analysed for all the simulations. The comparison of the assembly warpage does not show significant differences with a maximal variation of 0.1 μm .

The most important influence of solder ball stiffness is in the stresses generated in the BGA: Fig. 6 show six representations of the von Mises stress distribution in three balls from the centre on the left to the corner on the right with the same colour scale. The three first pictures are no IMC simulations and the last three are solder balls with 10 μm of IMC.

To achieve the evaluation of the IMC impact on thermomechanical loading of BGA in preparation of fatigue simulations, it is necessary to refine the mechanical analyses to a single solder ball. To that purpose, the technique of submodelling available in ABAQUS is used to properly export loads applied to the corner ball of a model with a finer mesh.

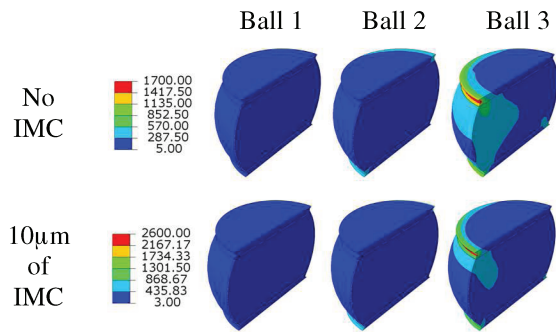


Fig. 6 : Von Mises stress (MPa) in 3 solder bumps from the centre to the corner of the BGA

Solder Mask Defined Ball investigations

Fig. 7 shows the Solder Mask Defined model of IMC in a single ball. To have smaller elements in the region of interest with the least of additional computational time, TIE constraints available in ABAQUS are used to ideally bond non coincident meshes of two different parts.

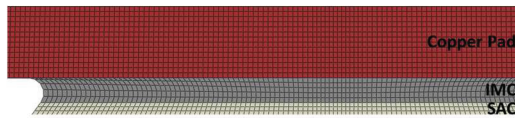


Fig. 7 : IMC mesh for SMD configuration

Copper pad, IMC layer and the early vicinity of solder constitute a single part where material properties are given to different sections of the same mesh. IMC thickness is changed manually in the definition of the model in function of the case to simulate. Three cases are considered: assemblies with no IMC, $5\mu\text{m}$ of IMC and $10\mu\text{m}$ of IMC.

As a first step, only solder bulk of the corner ball is analysed without the IMC layer and geometric singularity. It enables to compare the impact of the IMC thickness on the global loading of the ball with no parasite overwhelming stress divergence. Maximum von Mises stress level and location are compared for all the cases. The same thing is performed for peeling and shear stress. Fig. 8 shows the stress distributions of interest. The stress gradients do not change in shape but in magnitude. Stress and strain transferred to this part of the solder bump follow a uniform increase in function of the IMC without modifying the distribution (max and min locations etc.).

Analysis of the region near the bi-material IMC / Copper Pad was made separately (Fig. 9 and Fig. 10). The colour scale was referenced from the no IMC case in a way that makes appear in grey and black all the sites going beyond the initial limits. Black dash lines represent the bi-material interface in the cases of $5\mu\text{m}$ and $10\mu\text{m}$ of IMC.

Fig. 9 shows normal stress across the bump upper layer at the copper pad junction. The corner ball model was cut in half following the assembly diagonal in order to get stress values representative of the global load because of symmetry. First, the geometric singularity at the border of the junction modelled by a circle carries most of the maximum stresses. Even for a material transition away from this geometric artefact, stress is concentrated around

it. The thickest the IMC layer is, the more the singularity is loaded.

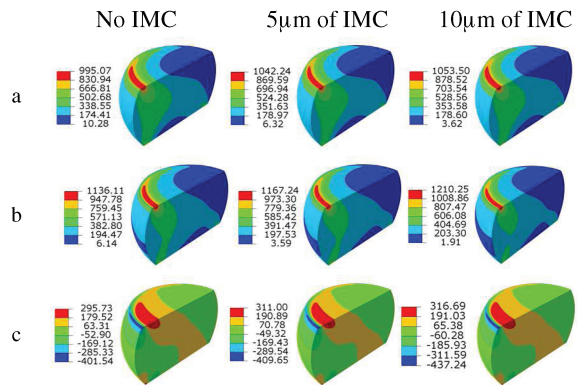


Fig. 8 : Stress distribution (MPa) in SMD balls (a) von Mises stress ; (b) normal tensile stress ; (c) shear stress

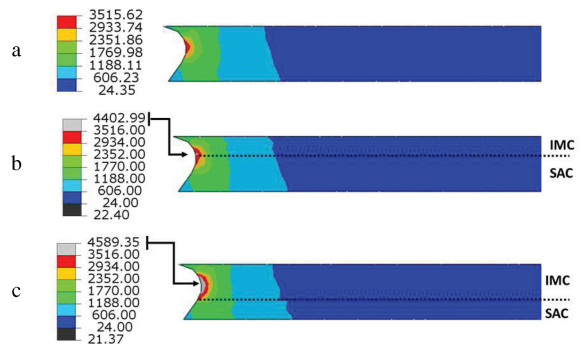


Fig. 9 : Normal stress (MPa) of the junction upper region for SMD: (a) no IMC ; (b) $5\mu\text{m}$ of IMC ; (c) $10\mu\text{m}$ of IMC

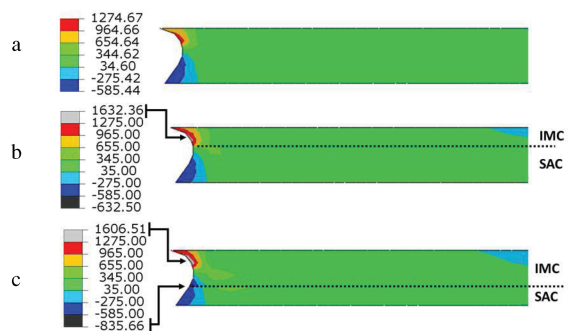


Fig. 10 : Shear stress (MPa) of the junction upper region for SMD: (a) no IMC ; (b) $5\mu\text{m}$ of IMC ; (c) $10\mu\text{m}$ of IMC

Then, the repeated colour scale shows how stress gradients are perturbed with the presence of IMC. Likewise the rest of the ball, stress levels increase with the IMC thickness but the distribution also changes beyond the IMC – solder bi-material interface. The same thing is observed in shear. It is explained by the discontinuity in the mechanical properties of the volume. Even if simulations are limited to treat this phenomenon, it can be characterised by evaluating the difference in stress between the two media. This gap is representative of a certain risk of crack initiation because it is distributed in the non-homogenous volume right next to the IMC and can lead to a stress concentration around a singular point. The difference in stress from one layer to another is plotted with respect to

the horizontal axis of the interface at the diagonal cut of the ball in Fig. 11.

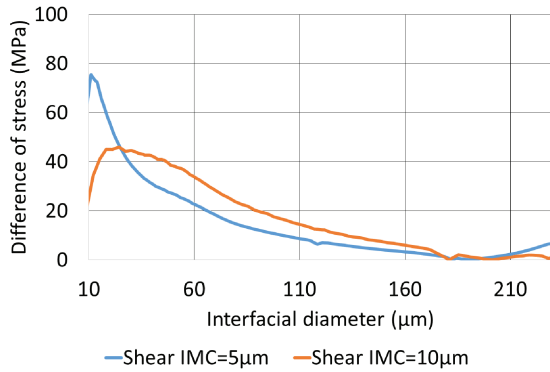


Fig. 11 : Interfacial gradient of stress

Gradients of stress at the frontier of the two materials (IMC and solder SAC) are more elevated in the exterior part of the ball even before approaching the singularity. It means there are higher risks for this region to initiate a crack coupled to the geometric singularity of the junction. One can notice that the divergence is higher in the 5μm case. It can be explained by the localisation of the bi-material interface right at the singularity. Except this numerical artefact, the gap of shear stress is smaller in this case than for 10μm of IMC.

Non Solder Mask Defined Ball investigations

The second configuration to be analysed is known as Non Solder Mask Defined soldering. Fig. 12 shows the model made in ABAQUS with the region of interest densely meshed.

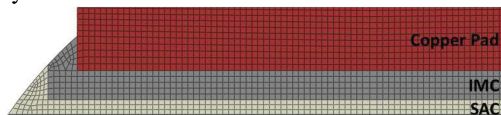


Fig. 12: IMC mesh for NSMD configuration

The same method is employed to study the impact of IMC layer on the NSMD balls loading. Von Mises stress, normal stress and shear stress distributions in the solder bulk without bi-material regions are shown in Fig. 13.

First, the distribution of the stress gradients is unchanged once again. Maxima and minima locations are the same from one case to another. Nevertheless, contrary of the SMD configuration, stress gradient levels decrease with the IMC thickness. It can be explained by considering the whole assembly subjected to differential strain. Unlike the previous SMD configuration, no geometric singularity overwhelms the rest of the ball. When the solder bump becomes stiffer, a larger part of the joint is solicited rather than concentrating stress at geometric singularity. Much of the loads are carried by the region of junction much stiffer.

The stress in the IMC layer is analysed by the same method as previously as shown in Fig. 14. Tensile stress increases for reduced sections at the upper sides of the junction. Once again, stress gradients are modified due to bi-material discontinuity.

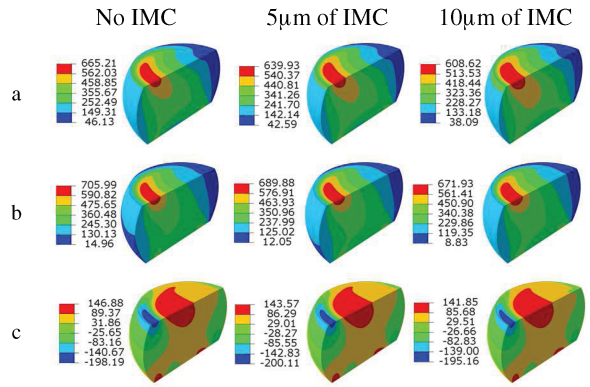


Fig. 13 : Stress distribution (MPa) in NSMD balls (a) von Mises stress ; (b) normal tensile stress ; (c) shear stress

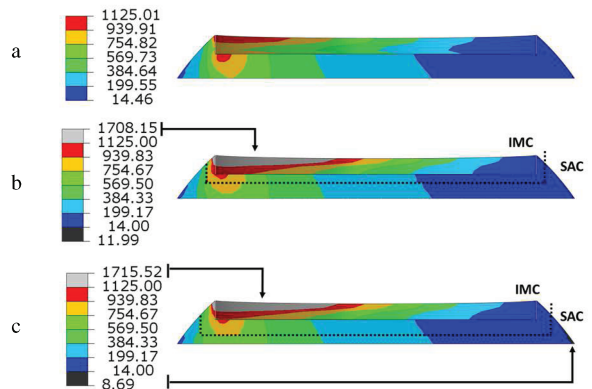


Fig. 14 : Normal stress (MPa) of the junction upper region for NSMD: (a) no IMC ; (b) 5μm of IMC ; (c) 10μm of IMC

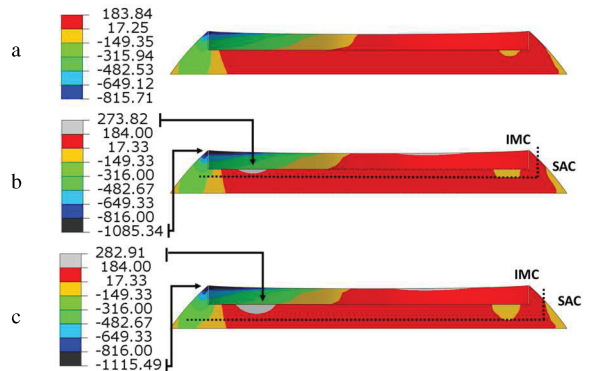


Fig. 15 : Shear stress (MPa) of the junction upper region for NSMD: (a) no IMC ; (b) 5μm of IMC ; (c) 10μm of IMC

Shear stress analysis leads to the same observations (Fig. 15). The location of maximum stress (colour grey) is not at an angle but at the copper pad junction embedded in the IMC layer on a third of the diameter of the ball.

To evaluate the risk of stress concentration right at the IMC frontier, the difference in shear stress between the two media is analysed. It goes from 40 to 60 MPa and is limited to the first third of the interface in diagonal. Moreover, as no nearby geometric singularity drives the local loading, the case with 10μm of IMC presents a discontinuity with a higher gap of stress that can initiate cracks at the interface.

Conclusions

Two numerical studies have been carried out to highlight the impact of IMC thickness on the mechanical response of a solder joint. Even in working in the elastic domain of the assembled materials, it has been shown that IMC layers play a role in characterisation of the material behaviour as well as in stress concentration in a BGA.

The FE analysis performed on the model of a SLS test with grooves showed that a non-critical error is expected on the Young's modulus and the creep properties of the material in using an extensometer. However, the more the solder joint tested becomes stiff, the more the whole assembly will experience tensile loading and thus leads to estimation error. It has to be taken into account during the tests. For example, if the solder joint is too thin, an adapted instrumentation have to be used like image correlation or gauges bonded on a specific device [18]. Nevertheless, solder materials are less stiff at high temperatures more subject to creep. Thus these precautions do not seem necessary in an oven. The IMC thickness should be measured for all the specimens in order to add a correction factor to the results.

The finite element analyses carried out on a BGA model of 144 balls showed an influence of IMC at the interfaces at several levels. First, the growth of IMC induces an increase in the solder stiffness of more than 15% depending on the amount of IMC considered at the interfaces. It justifies the need to model IMC layers in the assembly model and not only at the solder ball level. As the whole BGA stiffness increases and despite a global warpage unchanged, the stress in the corner ball varies significantly. The gradients across the corner ball present a discontinuity at the IMC – solder interface that depends on the IMC thickness. This can become a source of concern if such solicitations are concentrated at some point at the interfaces known for their irregular shape. This can become the driving parameter of fatigue generation and thus justifies the IMC layer implementation in the FE models.

Acknowledgments

This project is sponsored by Airbus Operations, Airbus Group Innovations, Continental Automotive France, Hirex Engineering, Labinal Power Systems, Nexio, Thales Alenia Space France, Thales Avionics and French National Agency for Research (ANR).

Special thanks to Michel Aussel from Continental Automotive France and Jérôme Parain from Thales Alenia Space France.

References

[1] European Parliament, "Directive 2011/65/EU of the European Parliament and of the Council of 8 June 2011 on the restriction of the use of certain hazardous substances in electrical and electronic equipment (RoHS)," *Off. J. Eur. Union*, 54, N°1; pp. 88–110, 2011.

[2] W. Lee, L. Nguyen, G. Selvaduray, "Solder joint fatigue models: review and applicability to chip scale packages," *Microelectron. Reliab.*, 40, N°2, pp. 231–244, 2000.

[3] H. Fremont, "How to combine experiments and simulations to study thermo-mechanical issues in complex microelectronics assemblies," *EuroSimE* 2010.

[4] H. Ma, J.C. Suhling, P. Lall, M.J. Bozack, "Reliability of the aging lead free solder joint," *ECTC*, 2006.

[5] H.L.J. Pang, K.H. Tan, X.Q. Shi, Z.P. Wang, "Microstructure and intermetallic growth effects on shear and fatigue strength of solder joints subjected to thermal cycling aging" *Mater. Sci. Eng. A*, 307, N°1–2, pp. 42–50, 2001.

[6] J.H.L. Pang, K.H. Prakash, T.H. Low, "Isothermal and thermal cycling aging on IMC growth rate in Pb-free and Pb-based solder interfaces," *Itherm*, 2, pp.109-115, 2004.

[7] W.H. Chen, C.F. Yu, H.C. Cheng, Y.M. Tsai, S.T. Lu, "IMC growth reaction and its effects on solder joint thermal cycling reliability of 3D chip stacking packaging," *Microelectron. Reliab.*, 53, N°1, pp. 30-40, 2013.

[8] F. X. Che, J.H.L. Pang, "Characterization of IMC layer and its effect on thermomechanical fatigue life of Sn3.8Ag0.7Cu solder joints," *J. Alloys Compd.*, 541, pp. 6-13, 2012.

[9] F.X.Che, J.H.L. Pang, L.H. Xu, "IMC consideration in FEA simulation for Pb-free solder joint reliability" *Thermomechanical Phenomena in Electronic Systems - Intersociety Conference*, 2006.

[10] M. Pocheron, J.Y. Deletage, B. Plano, A. Guedon-Gracia, and H. Fremont, "Assessment of constitutive properties of solder materials used in surface-mount devices for harsh environment applications," *IEEE TDMR*, 15, N°3, pp. 443–457, 2015.

[11] N. Iosipescu, "New Accurate Procedure for Single Shear Testing of Metals," *J. Mater.*, 2, N°3, pp. 537–566, 1967.

[12] T. Reinikainen, E. Suhir, "Novel test methodology for the most consistent and accurate characterization of solder materials in electronics engineering," *ECTC*, 2009.

[13] S. Deplanque, W. Nuchter, B. Wunderle, H. Walter, and B. Michel, "Evaluation of the primary and secondary creep of SnPb solder joint using a modified grooved-lap test specimen," *EuroSimE* 2004

[14] S. Deplanque, W. Nüchter, M. Spraul, B. Wunderle, R. Dudek, and B. Michel, "Relevance of primary creep in thermo-mechanical cycling for life-time prediction in Sn-based solders," *EuroSimE* 2005

[15] R. R. Chromik, R. P. Vinci, S. L. Allen, and M. R. Notis, "Nanoindentation measurements on Cu–Sn and Ag–Sn intermetallics formed in Pb-free solder joints," *J. Mater. Res.*, vol. 18, no. 09, pp. 2251–2261, 2003.

[16] A. Guédon-Gracia, E. Woïrgard, and C. Zardini, "Reliability of lead-free BGA assembly: Correlation between accelerated ageing tests and FE simulations," *IEEE TDMR.*, 8, N° 3, pp. 449–454, 2008.

[17] S. Wiese, S. Rzepka, "Time-independent elastic-plastic behaviour of solder materials" *Microelectron. Reliab.*, 44, N°12, pp. 1893-1900, 2004.

[18] S. Kwon, B. Han, Y. Lee, "Advanced Micro Shear Testing For Solder Alloy Using Direct Local Measurement" *Ipack* 2003